Supplementary Material

Figure 1

S1= -0.065 −

0.614×log.sigma.3.0.mm.3D_glszm_LargeAreaLowGrayLevelEmphasis +

0.463×log.sigma.5.0.mm.3D_glrlm_HighGrayLevelRunEmphasis +

0.486×wavelet.LHH_firstorder_Variance +

0.866×wavelet.LHL_glrlm_LongRunEmphasis −

0.988×wavelet.LLL_firstorder_RootMeanSquared

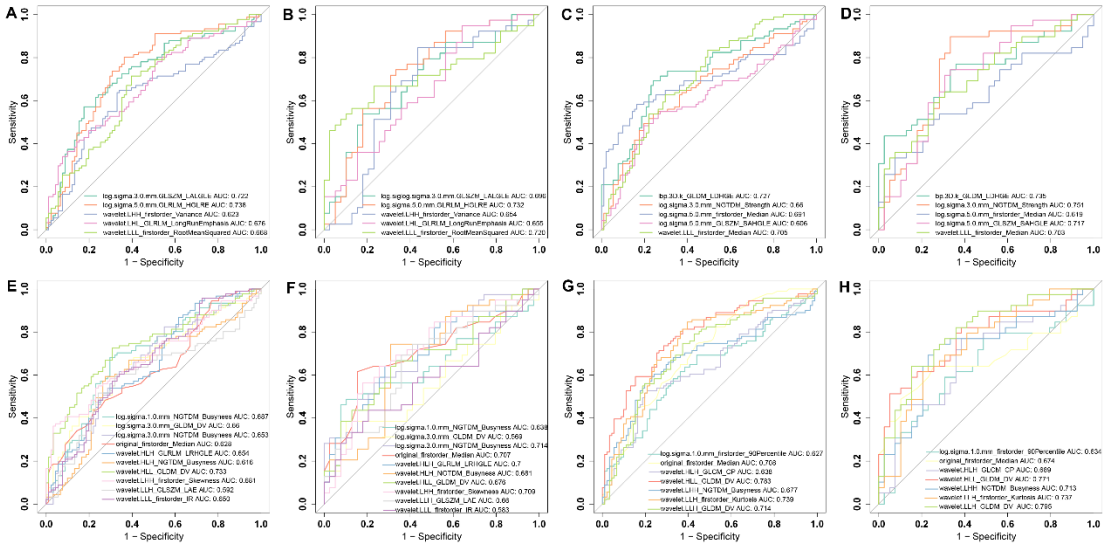

Figure 2 ROC curves of individual features in different models to identify squamous cell carcinoma of the esophagogastric junction (SCCEG) and adenocarcinoma of the esophagogastric junction (AEG) of the esophagogastric junction. 1A: ROC curves of individual features of 2D-arterial model identifying SCCEG and AEG in the training group; 1B: ROC curves of individual features of 2D-arterial model identifying SCCEG and AEG in the test group; 1C: ROC curves of individual features of 2D-venous model identifying SCCEG and AEG in the training group; 1D: ROC curves of individual features of 2D-venous model identifying SCCEG and AEG in the test group; 1E: ROC curves of individual features of 3D-arterial model identifying SCCEG and AEG in the training group; 1F: ROC curves of individual features of 3D-arterial model identifying SCCEG and AEG in the test group; 1G: ROC curves of individual features of 3D-venous model identifying SCCEG and AEG in the training group; 1H: ROC curves of individual features of 3D-venous model identifying SCCEG and AEG in the test group.

Figure 3

S2= 0.018 + 0.961×lbp.3D.k_gldm_LargeDependenceHighGrayLevelEmphasis + 0.542×log.sigma.3.0.mm.3D_ngtdm_Strength + 0.475×log.sigma.5.0.mm.3D_firstorder_Median + 0.413×log.sigma.5.0.mm.3D_glszm_SmallAreaHighGrayLevelEmphasis − 0.869×wavelet.LLL_firstorder_Median

Figure 4

S3= 0.266 − 0.852×log.sigma.1.0.mm.3D_ngtdm_Busyness + 0.708×log.sigma.3.0.mm.3D_gldm_DependenceVariance + 0.360×log.sigma.3.0.mm.3D_ngtdm_Busyness − 0.830×original_firstorder_Median − 1.160×wavelet.HLH_glrlm_LongRunHighGrayLevelEmphasis − 1.122×wavelet.HLH_ngtdm_Busyness + 0.656×wavelet.HLL_gldm_DependenceVariance + 0.715×wavelet.LHH_firstorder_Skewness + 2.398×wavelet.LLH_glszm_LargeAreaEmphasis + 0.777×wavelet.LLL_firstorder_InterquartileRange

Figure 5

S4= 0.047 + 0.760×log.sigma.1.0.mm.3D_firstorder_90Percentile − 1.030×original_firstorder_Median + 0.395×wavelet.HLH_glcm_ClusterProminence +

1.333×wavelet.HLL_gldm_DependenceVariance +

0.746×wavelet.LHH_ngtdm_Busyness +

0.381×wavelet.LLH_firstorder_Kurtosis +

0.409×wavelet.LLH_gldm_DependenceVariance

Figure 6

S5= $\text{Rad-score}^{AP\_VP\_2D} = -0.012 + 0.652\times\text{Rad-score}^{AP\_2D} + 0.786\times\text{Rad-score}^{VP\_2D}$

Figure 7

S6= $\text{Rad-score}^{AP\_VP\_3D} = 0.009 + 0.671\times\text{Rad-score}^{AP\_3D} + 0.621\times\text{Rad-score}^{VP\_3D}$

Table 1 The results of intra- and inter-observer ICCs for all the individual radiomics feature involved in the 2D-arterial model

Variable	Intra-observer ICCs	*P* value	Inter-observer ICCs	*P* value
log.sigma.3.0.mm.3D_glszm_LargeAreaLowGrayLevelEmphasis	0.920	7.25E-14	0.780	6.97E-08
log.sigma.5.0.mm.3D_glrlm_HighGrayLevelRunEmphasis	0.894	3.04E-12	0.835	6.65E-09
wavelet.LHH_firstorder_Variance	0.876	3.17E-11	0.770	2.39E-07
wavelet.LHL_glrlm_LongRunEmphasis	0.883	3.35E-11	0.853	3.14E-10
wavelet.LLL_firstorder_RootMeanSquared	0.866	1.21E-08	0.763	4.94E-07

ICCs: Intra-/inter-class correlation coefficient..

Table 2 The results of the multivariate logistic regression analysis for constructing the 2D-arterial model

Variable	B	Odds ratio (95%CI)	*P* value
Intercept	-0.065	0.937 (0.658-1.328)	0.715
log.sigma.3.0.mm.3D_glszm_ LargeAreaLowGrayLevelEmphasis	-0.614	0.541 (0.284-0.893)	0.040
log.sigma.5.0.mm.3D_glrlm_HighGrayLevelRunEmphasis	0.463	1.589 (1.050-2.577)	0.041
wavelet.LHH_firstorder_Variance	0.486	1.626 (1.100-2.474)	0.016
wavelet.LHL_glrlm_LongRunEmphasis	0.866	2.377 (1.550-3.786)	< 0.001
wavelet.LLL_firstorder_RootMeanSquared	-0.988	0.372 (0.232-0.566)	< 0.001

Table 3 Statistical differences analysis of radiomics features in 2D-arterial model and Rad-score^{AP_2D} between SCCEG groups and AEG in the training and test groups

Training group							
Variable	**Sample**	**AEG**		**SCCEG**		**Statistics**	***P* value**
log.sigma.3.0.mm.3D_glszm_LargeAreaLowGrayLevelEmphasis	182	-0.12	(-0.40, 0.34)	-0.46	(-0.49, -0.25)	5.179	< 0.001
log.sigma.5.0.mm.3D_glrlm_HighGrayLevelRunEmphasis	182	-0.60	(-0.69, -0.20)	0.02	(-0.50, 0.57)	-5.537	< 0.001
wavelet.LHH_firstorder_Variance	182	-0.16	(-0.58, 0.34)	-0.58	(-0.60, 0.04)	2.855	0.004
wavelet.LHL_glrlm_LongRunEmphasis	182	-0.39	(-1.17, 0.55)	0.52	(-0.43, 1.02)	-4.099	< 0.001
wavelet.LLL_firstorder_RootMeanSquared	182	0.19	(-0.55, 0.66)	-0.31	(-0.89, 0.18)	3.921	< 0.001
Rad-score^{AP_2D}	182	-0.46	(-1.40, -0.01)	0.78	(-0.02, 1.39)	-7.171	< 0.001
Test group							
Radiomics features	Sample	AEG		SCCEG		Statistics	*P* value
log.sigma.3.0.mm.3D_glszm_LargeAreaLowGrayLevelEmphasis	78	-0.25	(-0.44, 0.10)	-0.47	(-0.49, -0.28)	2.983	0.003
log.sigma.5.0.mm.3D_glrlm_HighGrayLevelRunEmphasis	78	-0.60	(-0.67, -0.19)	0.05	(-0.48, 0.48)	-3.523	< 0.001
wavelet.LHH_firstorder_Variance	78	-0.25	(-0.60, 0.04)	-0.60	(-0.60, -0.53)	2.343	0.019

wavelet.LHL_glrlm_LongRunEmphasis	78	0.03 (-1.11, 0.67)	0.34 (-0.38, 0.89)	-2.363	0.018
wavelet.LLL_firstorder_RootMeanSquared	78	0.26±0.74	-0.40±1.08	3.156	0.002
Rad-score^{AP_2D}	78	-0.67±1.18	0.67±1.44	-4.492	< 0.001

SCCEG: squamous cell carcinoma of the esophagogastric junction; AEG: adenocarcinoma of the esophagogastric junction; The variables without normal distribution were depicted by median (interquartile range, IQR); The variables with normal distribution were depicted by mean ± SD; Statistically significant level: $P < 0.05$

Table 4 The results of intra- and inter-observer ICCs for all the individual radiomics feature involved in the 2D-venous model

Variable	intra-observer ICCs	*P* value	inter-observer ICCs	*P* value
lbp.3D.k_gldm_LargeDependenceHighGrayLevelEmphasis	0.860	1.47E-10	0.765	4.09E-05
log.sigma.3.0.mm.3D_ngtdm_Strength	0.806	3.02E-08	0.751	4.65E-07
log.sigma.5.0.mm.3D_firstorder_Median	0.877	2.93E-11	0.780	7.18E-08
log.sigma.5.0.mm.3D_glszm_SmallArea HighGrayLevelEmphasis	0.796	6.03E-08	0.817	1.86E-07
wavelet.LLL_firstorder_Median	0.932	9.83E-15	0.860	2.52E-10

ICCs: Intra-/inter-class correlation coefficient.

Table 5 The results of the multivariate logistic regression analysis for constructing the 2D-venous model

Variable	B	Odds ratio (95%CI)	*P* value
Intercept	0.018	1.019 (0.706-1.473)	0.922
lbp.3D.k_gldm_LargeDependenceHighGrayLevelEmphasis	0.961	2.613 (1.784-3.980)	< 0.001
log.sigma.3.0.mm.3D_ngtdm_Strength	0.542	1.719 (1.010-3.113)	0.057
log.sigma.5.0.mm.3D_firstorder_Median	0.475	1.608 (1.029-2.611)	0.044
log.sigma.5.0.mm.3D_glszm_SmallAreaHighGrayLevelEmphasis	0.413	1.511 (0.881-2.766)	0.153
wavelet.LLL_firstorder_Median	-0.869	0.419 (0.260-0.643)	< 0.001

Table 6 Statistical differences analysis of radiomics features in 2D-venous model and Rad-score^{VP_2D} between SCCEG groups and AEG in the training and test groups

Training group						
Variable	**Sample**	**AEG**	**SCCEG**	**Statistics**	***P* value**
lbp.3D.k_gldm_LargeDependenceHighGrayLevelEmphasis	182	-0.44 (-1.02, -0.01)	0.45 (-0.42, 1.11)	-5.28	< 0.001
log.sigma.3.0.mm.3D_ngtdm_Strength	182	-0.60 (-0.67, -0.30)	-0.14 (-0.61, 0.74)	-3.736	< 0.001
log.sigma.5.0.mm.3D_firstorder_Median	182	0.00 (-0.32, 0.30)	0.45 (-0.17, 0.80)	-4.456	< 0.001
log.sigma.5.0.mm.3D_glszm_SmallAreaHighGrayLevelEmphasis	182	-0.44 (-0.59, -0.24)	-0.21 (-0.58, 0.49)	-2.469	0.014
wavelet.LLL_firstorder_Median	182	0.35 (-0.33, 0.97)	-0.39 (-0.86, 0.19)	4.774	< 0.001
Rad-score^{VP_2D}	182	-0.96±1.44	1.00±1.36	-9.461	< 0.001
Test group					
Variable	**Sample**	**AEG**	**SCCEG**	**Statistics**	***P* value**
lbp.3D.k_gldm_LargeDependenceHighGrayLevelEmphasis	78	-0.36±0.71	0.44±0.94	-4.25	< 0.001
log.sigma.3.0.mm.3D_ngtdm_Strength	78	-0.65 (-0.68, -0.34)	-0.33 (-0.55, 0.62)	-3.822	< 0.001
log.sigma.5.0.mm.3D_firstorder_Median	78	0.14 (-0.25, 0.30)	0.29 (0.01, 0.66)	-1.804	0.071
log.sigma.5.0.mm.3D_glszm_SmallAreaHighGrayLevelEmphasis	78	-0.51 (-0.61, -0.29)	-0.25 (-0.46, 0.11)	-3.293	0.001
wavelet.LLL_firstorder_Median	78	0.22±0.75	-0.41±0.82	3.531	0.001

Rad-scoreVP_2D	78	-0.77±1.26	0.91±1.20	-6.039	< 0.001

SCCEG: Squamous cell carcinoma of the esophagogastric junction; AEG: Adenocarcinoma of the esophagogastric junction; The variables without normal distribution were depicted by median (interquartile range, IQR); The variables with normal distribution were depicted by mean ± SD; Statistically significant level: $P < 0.05$

Table 7 The results of intra- and inter-observer ICCs for all the individual radiomics feature involved in the 3D-arterial model

Variable	intra-observer ICCs	*P* value	inter-observer ICCs	*P* value
log.sigma.1.0.mm.3D_ngtdm_Busyness	0.783	4.75E-06	0.754	1.32E-07
log.sigma.3.0.mm.3D_gldm_DependenceVariance	0.955	0.002316	0.752	2.78E-17
log.sigma.3.0.mm.3D_ngtdm_Busyness	0.968	1.31E-06	0.758	3.13E-19
original_firstorder_Median	0.989	6.91E-14	0.932	9.36E-26
wavelet.HLH_glrlm_LongRunHighGrayLevelEmphasis	0.904	3.94E-05	0.899	2.41E-12
wavelet.HLH_ngtdm_Busyness	0.825	3.77E-13	0.916	3.68E-09
wavelet.HLL_gldm_DependenceVariance	0.976	0.007624	0.869	5.65E-19
wavelet.LHH_firstorder_Skewness	0.938	1.04E-07	0.773	1.26E-15
wavelet.LLH_glszm_LargeAreaEmphasis	0.951	3.24E-20	0.973	5.37E-17
wavelet.LLL_firstorder_InterquartileRange	0.931	0.035596	0.752	6.70E-15

ICCs: intra-/inter-class correlation coefficient (ICCs)

Table 8 The results of the multivariate logistic regression analysis for constructing the 3D-arterial model

Variable	B	Odd ratio (95%CI)	*P* value
Intercept	0.266	1.305 (0.829-2.115)	0.262
log.sigma.1.0.mm.3D_ngtdm_Busyness	-0.852	0.427 (0.170-0.876)	0.041
log.sigma.3.0.mm.3D_gldm_DependenceVariance	0.708	2.030 (1.180-3.624)	0.013
log.sigma.3.0.mm.3D_ngtdm_Busyness	0.360	1.433 (0.872-2.316)	0.144
original_firstorder_Median	-0.830	0.436 (0.254-0.700)	0.001
wavelet.HLH_glrlm_LongRunHighGrayLevelEmphasis	-1.160	0.313 (0.147-0.610)	0.001
wavelet.HLH_ngtdm_Busyness	-1.122	0.326 (0.132-0.754)	0.010
wavelet.HLL_gldm_DependenceVariance	0.656	1.927 (1.196-3.260)	0.010
wavelet.LHH_firstorder_Skewness	0.715	2.045 (1.013-4.569)	0.061
wavelet.LLH_glszm_LargeAreaEmphasis	2.398	11.000 (2.503-61.744)	0.003
wavelet.LLL_firstorder_InterquartileRange	0.777	2.174 (1.346-3.690)	0.002

Table 9 Statistical differences analysis of radiomics features in 3D-arterial model and Rad-score^{AP_3D} between SCCEG groups and AEG in the training and test groups

Training group					
Variable	**Sample**	**AEG**	**SCCEG**	**Statistics**	***P* value**
log.sigma.1.0.mm.3D_ngtdm_Busyness	182	-0.14 (-0.45, 0.44)	-0.48 (-0.64, -0.14)	4.346	< 0.001
log.sigma.3.0.mm.3D_gldm_DependenceVariance	182	-0.33 (-0.85, 0.20)	0.14 (-0.49, 0.89)	-3.733	< 0.001
log.sigma.3.0.mm.3D_ngtdm_Busyness	182	-0.19 (-0.59, 0.69)	-0.57 (-0.71, -0.16)	3.564	< 0.001
original_firstorder_Median	182	0.08 (-0.45, 0.83)	-0.26 (-0.81, 0.42)	2.990	0.003
wavelet.HLH_glrlm_LongRunHighGrayLevelEmphasis	182	-0.27 (-0.69, 1.03)	-0.68 (-0.71, 0.16)	3.578	< 0.001
wavelet.HLH_ngtdm_Busyness	182	-0.49 (-0.52, -0.27)	-0.32 (-0.50, 0.19)	-2.700	0.007
wavelet.HLL_gldm_DependenceVariance	182	-0.39±0.82	0.39±1.01	-5.753	< 0.001
wavelet.LHH_firstorder_Skewness	182	-0.46 (-0.52, -0.30)	-0.26 (-0.49, 0.78)	-4.220	< 0.001
wavelet.LLH_glszm_LargeAreaEmphasis	182	-0.34 (-0.36, -0.28)	-0.24 (-0.36, 0.17)	-2.146	0.032
wavelet.LLL_firstorder_InterquartileRange	182	-0.32 (-1.06, 0.14)	0.05 (-0.41, 0.74)	-3.491	< 0.001
Rad-score^{AP_3D}	182	-1.17 (-2.47, -0.53)	1.30 (0.24, 3.74)	-8.764	< 0.001
Test group					
Variable	**Sample**	**AEG**	**SCCEG**	**Statistics**	***P***

	le				cs	value
log.sigma.1.0.mm.3D_ngtdm_Busyness	78	-0.12	(-0.44, 0.38)	-0.51	(-0.69, 0.14)	2.104	0.035
log.sigma.3.0.mm.3D_gldm_DependenceVariance	78	-0.30±0.96		0.04±1.42		-1.264	0.211
log.sigma.3.0.mm.3D_ngtdm_Busyness	78	-0.07	(-0.47, 0.86)	-0.53	(-0.80, 0.05)	3.253	0.001
original_firstorder_Median	78	0.22	(-0.04, 0.63)	-0.33	(-1.25, 0.33)	3.143	0.002
wavelet.HLH_glrlm_LongRunHighGrayLevelEmphasis	78	-0.24	(-0.70, 0.55)	-0.70	(-0.72, -0.24)	3.043	0.002
wavelet.HLH_ngtdm_Busyness	78	-0.46	(-0.52, 0.13)	-0.20	(-0.46, 0.49)	-2.753	0.006
wavelet.HLL_gldm_DependenceVariance	78	-0.21±0.67		0.31±0.86		-2.989	0.004
wavelet.LHH_firstorder_Skewness	78	-0.40	(-0.50, -0.23)	-0.05	(-0.39, 0.52)	-3.183	0.001
wavelet.LLH_glszm_LargeAreaEmphasis	78	-0.33	(-0.35, -0.09)	-0.24	(-0.32, 0.70)	-2.433	0.015
wavelet.LLL_firstorder_InterquartileRange	78	-0.30	(-0.88, -0.03)	-0.16	(-0.78, 0.94)	-1.254	0.210
Rad-scoreAP_3D	78	-1.12	(-2.56, -0.20)	1.22	(-0.73, 2.84)	-4.932	< 0.001

SCCEG: Squamous cell carcinoma of the esophagogastric junction; AEG: Adenocarcinoma of the esophagogastric junction; The variables without normal distribution were depicted by median (interquartile range, IQR); The variables with normal distribution were depicted by mean ± SD; Statistically significant level: $P < 0.05$.

Table 10 The results of intra- and inter-observer ICCs for all the individual radiomics feature involved in the 3D-venous model

Variable	Intra-observer ICCs	*P* value	Inter-observer ICCs	*P* value
log.sigma.1.0.mm.3D_firstorder_90Percentile	0.961	0.00012	0.914	1.90E-09
original_firstorder_Median	0.986	2.66E-08	0.883	9.51E-25
wavelet.HLH_glcm_ClusterProminence	0.910	8.44E-13	0.906	3.75E-13
wavelet.HLL_gldm_DependenceVariance	0.969	4.36E-06	0.924	4.02E-20
wavelet.LHH_ngtdm_Busyness	0.981	6.13E-09	0.829	4.07E-22
wavelet.LLH_firstorder_Kurtosis	0.849	8.22E-11	0.875	1.49E-08
wavelet.LLH_gldm_DependenceVariance	0.970	2.09E-15	0.946	4.47E-20

ICCs: Intra-/inter-class correlation coefficient.

Table 11 The results of the multivariate logistic regression analysis for constructing the 3D-venous model

Variable	B	Odds ratio (95%CI)	*P* value
Intercept	0.047	1.048 (0.709-1.558)	0.815
log.sigma.1.0.mm.3D_firstorder_90Percentile	0.760	2.138 (1.255-3.887)	0.008
original_firstorder_Median	-1.030	0.357 (0.212-0.565)	< 0.001
wavelet.HLH_glcm_ClusterProminence	0.395	1.484 (0.952-2.892)	0.140
wavelet.HLL_gldm_DependenceVariance	1.333	3.794 (2.212-7.046)	< 0.001
wavelet.LHH_ngtdm_Busyness	0.746	2.108 (1.233-4.219)	0.016
wavelet.LLH_firstorder_Kurtosis	0.381	1.464 (0.901-2.48)	0.136
wavelet.LLH_gldm_DependenceVariance	0.409	1.506 (0.875-2.625)	0.141

Table 12 Statistical differences analysis of radiomics features in 3D-venous model and Rad-score^{VP_3D} between SCCEG groups and AEG in the training and test groups

Variable	Sample	AEG	SCCEG	Statistics	*P* value
log.sigma.1.0.mm.3D_firstorder_90Percentile	182	0.12 (-0.54, 0.72)	-0.48 (-0.94, 0.49)	2.962	0.003
original_firstorder_Median	182	0.24 (-0.39, 0.94)	-0.34 (-0.91, 0.22)	4.836	< 0.001
wavelet.HLH_glcm_ClusterProminence	182	-0.24 (-0.28, -0.09)	-0.29 (-0.29, -0.18)	3.218	0.001
wavelet.HLL_gldm_DependenceVariance	182	-0.46±0.75	0.46±1.01	-6.901	< 0.001
wavelet.LHH_ngtdm_Busyness	182	-0.50 (-0.52, -0.43)	-0.22 (-0.51, 0.60)	-4.124	< 0.001
wavelet.LLH_firstorder_Kurtosis	182	-0.72 (-0.83, -0.29)	0.05 (-0.54, 1.10)	-5.567	< 0.001
wavelet.LLH_gldm_DependenceVariance	182	-0.39 (-0.99, 0.31)	0.55 (-0.16, 0.90)	-4.985	< 0.001
Rad-score^{VP_3D}	182	-1.29±1.54	1.39±1.70	-11.159	< 0.001
Test group					
Variable	**Sample**	**AEG**	**SCCEG**	**Statistics**	***P* value**
log.sigma.1.0.mm.3D_firstorder_90Percentile	78	0.29 (-0.63, 0.69)	-0.52 (-1.10, 0.20)	2.044	0.041
original_firstorder_Median	78	-0.02 (-0.26, 0.43)	-0.46 (-1.30, 0.30)	2.643	0.008
wavelet.HLH_glcm_ClusterProminence	78	-0.25 (-0.29, -0.09)	-0.29 (-0.29, -0.27)	2.873	0.004

wavelet.HLL_gldm_DependenceVariance	78	-0.28	(-0.75, 0.15)	0.62	(-0.16, 1.00)	-4.122	< 0.001
wavelet.LHH_ngtdm_Busyness	78	-0.46	(-0.51, -0.33)	-0.06	(-0.42, 1.12)	-3.233	0.001
wavelet.LLH_firstorder_Kurtosis	78	-0.49	(-0.76, -0.09)	0.04	(-0.34, 0.86)	-3.603	< 0.001
wavelet.LLH_gldm_DependenceVariance	78	-0.31±0.75		0.50±0.66		-5.072	< 0.001
Rad-score^{VP_3D}	78	-0.81±1.36		1.87±1.80		-7.403	< 0.001

SCCEG: Squamous cell carcinoma of the esophagogastric junction; AEG: Adenocarcinoma of the esophagogastric junction; The variables without normal distribution were depicted by median (interquartile range, IQR); The variables with normal distribution were depicted by mean ± SD; Statistically significant level: $P < 0.05$.

Table 13 The results of Delong test for AUC values of paired models

	Training group		Test group	
Models	*Z*	***P* value**	***Z***	***P* value**
2D-arterial model.*vs*2D-venous model	-1.105	0.269	-1.253	0.210
2D-arterial model.*vs*3D-venous model	-2.027	0.043	-1.199	0.231
2D-arterial model.*vs*3D-venous model	-1.814	0.070	-1.981	0.048
2D-arterial model.*vs*2D-combined model	-2.514	0.012	-2.332	0.020
2D-arterial model.*vs*3D-combined model	-2.809	0.005	-2.495	0.013
2D-venous model.*vs*3D-arterial model	-0.890	0.374	0.117	0.907
2D-venous model.*vs*3D-venous model	-1.036	0.300	-0.959	0.337
2D-venous model.*vs*2D-combined model	-1.382	0.167	-0.517	0.605
2D-venous model.*vs*3D-combined model	-2.050	0.040	-1.503	0.133
3D-arterial model.*vs*3D-venous model	-0.041	0.967	-1.150	0.250
3D-arterial model.*vs*2D-combined model	0.255	0.799	-0.402	0.688
3D-arterial model.*vs*3D-combined model	-1.770	0.076	-2.459	0.014
3D-venous model.*vs*2D-combined model	0.296	0.767	0.714	0.475
3D-venous model.*vs*3D-combined model	-2.019	0.043	-1.060	0.288
2D-combined model.*vs*3D-combined model	-1.397	0.163	-1.277	0.202

Statistically significant level: $P < 0.05$.

Table 14 Continuous NRI and IDI for the different radiomics models to differentiate SCCEG and AEG

	Training group				Test group			
Models	**NRI (95% CI)**	***P* value**	**IDI (95% CI)**	***P* value**	**NRI (95% CI)**	***P* value**	**IDI (95% CI)**	***P* value**
2D-arterial model *vs* 2D-combined model	0.747 (0.478-1.017)	0.000	0.131 (0.082-0.179)	0.000	1.128 (0.762-1.495)	0.000	0.126 (0.063-0.190)	< 0.001
2D-venous model *vs* 2D-combined model	0.637 (0.363-0.912)	< 0.001	0.050 (0.016-0.084)	0.004	0.462 (0.032-0.891)	0.035	0.008 (-0.050-0.067)	0.779
2D-arterial model *vs* 3D-arterial model	0.571 (0.297-0.846)	< 0.001	0.160 (0.082-0.237)	< 0.001	0.513 (0.084-0.942)	0.019	0.110 (-0.004-0.224)	0.058
2D-venous model *vs* 3D-venous model	0.308 (0.023-0.593)	0.034	0.079 (0.006-0.151)	0.033	0.513 (0.088-0.938)	0.018	0.122 (0.003-0.241)	0.045
3D-arterial model *vs* 3D-combined model	0.550 (0.271-0.828)	< 0.001	0.072 (0.035-0.109)	< 0.001	0.974 (0.587-1.361)	0.000	0.168 (0.107-0.229)	0.000
3D-venous model *vs* 3D-combined	0.791 (0.525-1.0	0.000	0.072 (0.034-0.111)	< 0.001	0.359 (-0.077-0.	0.107	0.039 (-0.036-0.1	0.314

model		58)				795)		13)	
2D-combined model	*vs*	0.506	<	0.101		0.718	0.00	0.152	
3D-combined model		(0.226-0.786)	0.001	(0.030-0.172)	0.006	(0.305-1.131)	1	(0.041-0.263)	0.007

Continuous NRI: Continuous net reclassification improvement; NRI: Integrated discrimination improvement; Statistically significant level: $P < 0.05$.

Table 15 The results of the Hosmer-Lemeshow test for different radiomics models in the training and test groups

	Training group		Test group	
Models	**Statistics**	***P* value**	**Statistics**	***P* value**
2D-arterial model	9.656	0.290	7.952	0.438
2D-venous model	13.562	0.094	12.060	0.149
3D-arterial model	5.914	0.657	11.324	0.184
3D-venous model	6.466	0.595	9.968	0.267
2D-combined model	12.781	0.120	11.630	0.168
3D-combined model	4.099	0.848	6.965	0.540

The model has superior goodness of fit: $P > 0.05$.